

MULTI OBJECTIVE OPTIMIZATION FOR HOUSE ROOF USING ARTIFICIAL NEURAL NETWORK MODEL

Ali Habeeb Askar 

*PhD student, University of Miskolc, Department of Fluid and Heat Engineering
Institute of Physics and Electric Engineering*

*Mechanical Engineering Department, University of Technology – Iraq, Baghdad 10066, Iraq
3515 Miskolc-Egyetemváros, e-mail: 20156@uotechnology.edu.iq*

Endre Kovács 

*associate professor, University of Miskolc, Institute of Physics and Electric Engineering
3515 Miskolc-Egyetemváros, e-mail: fizendre@uni-miskolc.hu*

Betti Bolló 

*associate professor, University of Miskolc, Department of Fluid and Heat Engineering
3515 Miskolc-Egyetemváros, e-mail: betti.bollo@uni-miskolc.hu*

Abstract

Roof models with low heat loss and low heating costs for buildings are crucial for reducing energy consumption and greenhouse gas emissions in cold regions. This study aimed to calculate the heat loss for various roof models with low heat loss, which are widely used in houses in Europe and other cold regions. We created 324 models for three types of roofs (light, medium, and heavy) with different materials and thicknesses using the HAP program. We then trained a neural network (ANN) to generate a mathematical function that can be used to calculate the optimal surface using a multi-objective genetic algorithm method. The resulting optimal roof design was simulated using the Ansys program on a January day. We compared the heat loss results for the optimal roof for HAP, ANN, and transient thermal analysis by Ansys, respectively, showing a close agreement among the methods.

Keywords: *multi-objective genetic algorithm, roof design, optimization, heating load, insulated roof*

1. Introduction

Energy consumption is a subject of global debate, with the construction and dwelling sectors accounting for 36% of global energy consumption and 37% of carbon dioxide emissions in 2020. Climate change and population growth are expected to increase energy demand between 2010 and 2050, with projected values of 80% and 83%, respectively. Heat loss through building walls is higher when the roof area is smaller (Zingre et al., 2017). Since all heat transmission mechanisms are present and building components have several layers of different materials, thermal analysis of a complete structure is complicated and time-consuming. The design parameters are sometimes time-dependent since factors like ambient temperature, wind velocity, and sun irradiation vary. In addition to ventilation and infiltration, heat gains from occupancy, equipment use, lighting, and solar radiation via fenestration must be considered. Thus, several methods exist to estimate a structure's energy usage (Al-Sanea, 2002). The Designer must consi-

der temperature fluctuations in walls and roofs to determine heating and cooling loads, considering internal and exterior conditions (Höglund et al., 1967). Previous research into surface characteristics has shown a number of methods for making use of surface qualities to improve the efficiency and longevity of building envelopes (Imran et al., 2018). The impact of coatings' solar reflectances and infrared emittances on the thermal performance of roofs protected by the coatings (Wilkes et al., 1997). In winter, the temperature of the roof surface tends to decrease due to the presence of cold air and the low intensity of solar radiation. The described phenomenon imposes a lost thermal load on the area as a result of the external radiation of heat emanating from the surface (Petter et al., 2015; Chen and Lu, 2021; Santamouris et al., 2011). Also, technologies that are used to reduce the cooling load in the summer are now unfavourable for use in cold regions, and, on the contrary, dissimilar radiation characteristics are now favourable. In order to reduce the heating requirements of the structure, it is desirable to increase its absorption of short waves. In areas with low temperatures, it is common to apply black paint to the roofs and other external surfaces of buildings. Hong et al. (Hong et al., 2022) conducted a field study, to measure the surface temperatures of buildings of different colours. Diverse surface colours have been found, which, in turn, lead to a diverse absorption of short waves and significant temperature changes on the Earth's surface. High absorption of short waves has been shown to be beneficial during the winter, especially in very cold regions. According to Britain et al. (Nowak, 1991), the net radiative heat loss of surfaces is significantly affected by long-wave radiation. In addition, the energy consumption of buildings is affected by both the emissivity of long-wave radiation and the absorption of short-wave radiation in the envelopes of buildings, as mentioned in the reference (Shi and Zhand, 2011). The ideal way to reduce the amount of heat required during the winter is to use a material that exhibits high short-wave absorptivity and low long-wave emissivity. The roof structure shows a multitude of potentials, including shielding against rainfall and allowing for the entry of daylight while preventing the direct transmission of solar radiation (shortwave radiation) into the indoor space during daylight hours (Chantawong, 2017).

Carrier's Hourly Analysis Programme (HAP) is a multipurpose software package with extensive energy analysis tools for evaluating the efficiency and cost-effectiveness of potential HVAC system designs for commercial buildings. By combining these two tools into one convenient bundle, considerable time savings are achieved. It may be possible to use the input data and results from system design simulations in energy assessments with no further tweaks (carrier.com). So that we can use this tool to collect the data by setting the weather data for Miskolc city Hungary, choosing the space, putting the type of roof for that space, and taking only the heat loss through the roof for the design condition in each model to collect the data that will be used to build a neural network.

Various techniques exist for constructing multi-variable linear or nonlinear prediction models, including regression polynomials such as ARMA (Kho et al., 2002), Artificial Neural Network (ANN) (Moayed et al., 2019), and Inverse Distance Weighting (IDW) (Lu and Wong, 2008). There is an increasing trend of individuals directing their focus towards Artificial Neural Networks (ANN) in particular (Jang et al., 2019). The training of input-output pairs from tests is utilised to depict intricate and nonlinear functional relationships among numerous parameters. The multi-layered perceptron of Artificial Neural Networks (ANN) can be likened to a multi-mapping black box analysis function (Gardner and Dorling, 1998). Artificial Neural Networks (ANN) have been effectively utilised in a variety of applications due to their flexible characteristics and capacity for self-learning, including predicting indoor temperature (Pandey et al., 2012), heat radiation modelling (Tausendschön and Radl, 2021), optimizing the energy efficiency of residential buildings (Gao, 2022), and predicting temperature distribution (Askar et al., 2021).

This work, as all calculation procedures involve some assumptions, the accuracy of any method must ultimately be established by comparing the results of calculations with experimental results and simulations performed by Ansys. Where the heat losses were calculated for several models of the roof, and after collecting the data using the HAP programme, a neural network model was built and used with the multi-objective Genetic algorithm method to reach the optimal model of the roof in terms of heat losses and cost. A simulation is then carried out for these selected models.

2. Methodology

2.1. The Models of Roofs

The model consists of a room in which all walls and the ceiling are exposed to the outside, located in the city of Miskolc, Hungary, with a latitude of 48.1 and a longitude of 20.7. The dimensions of the room are 5 metres wide, 5 metres long, and 3 metres high. The thermal losses of the roof were practically calculated using the HAP program using three types of roofs (light weight roof, medium weight roof, and heavy weight roof) as shown in Fig. 1, where each roof has six layers (Acoustic tile, Ceiling air space, concrete, insulation, felt-membrane, and slag or stone) of different materials: layer one for soundproofing, layer two air gap is used to reduce heat loss, as well as to serve the passage of other structures of the building. Layers three and four we will concentrate on them because they are more important for the heat loss: the concrete and insulation layers. Layer five is the moisture-proof layer, and the last layer is the outer layer to cover the roof and save the other layers from the weather conditions. Emphasis was placed on the lost heat through the roof to generate input and output data by changing the type of materials for the roof layers as well as the thickness of each layer. Table 1 represents the materials used as well as the thickness of each layer.

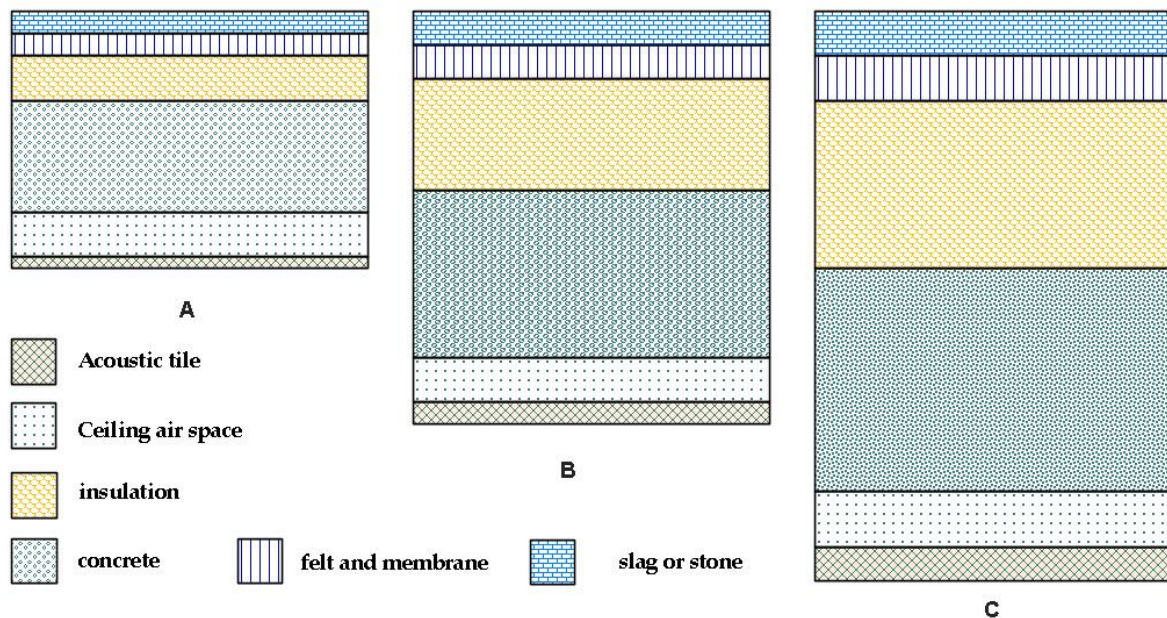


Figure 1. Show the three type of roof (A)light weight roof, (B) Medium weight roof, and (C) heavy weight roof

Table 1. The materials used with the thickness of each layer

Roof type	Number of layer	Type of material	Thickness of the layer [mm]	
Light weight roof	<i>Layer one</i>	Acoustic tile	5, 10 and 15	
	<i>Layer two</i>	Ceiling air space	150	
	<i>Layer three</i>	<i>LW concrete</i>		50, 75 and 100
		<i>LW concrete block</i>		50, 75 and 100
		<i>face brick</i>		50, 75 and 100
		<i>common brick</i>		50, 75 and 100
<i>Layer four</i>	<i>RSI-1.2board insulation</i>		20,30, and 40	
<i>Layer five</i>	<i>felt and membrane</i>		10	
<i>Layer six</i>	<i>slag or stone</i>		10	
Medium weight roof	<i>Layer one</i>	Acoustic tile	20, 25 and 30	
	<i>Layer two</i>	Ceiling air space	200	
	<i>Layer three</i>	<i>HW concrete</i>		100, 125 and 150
		<i>HW concrete block</i>		100, 125 and 150
		<i>face brick</i>		100, 125 and 150
		<i>common brick</i>		100, 125 and 150
<i>Layer four</i>	<i>RSI-3.3 batt insulation</i>		100,150, and 200	
<i>Layer five</i>	<i>felt and membrane</i>		15	
<i>Layer six</i>	<i>slag or stone</i>		15	
Heavy weight roof	<i>Layer one</i>	Acoustic tile	30, 35 and 40	
	<i>Layer two</i>	Ceiling air space	250	
	<i>Layer three</i>	<i>HW concrete</i>		150, 200 and 250
		<i>HW concrete block</i>		150, 200 and 250
		<i>face brick</i>		150, 200 and 250
		<i>common brick</i>		150, 200 and 250
<i>Layer four</i>	<i>RSI-6.7 batt insulation</i>		200,250, and 300	
<i>Layer five</i>	<i>felt and membrane</i>		20	
<i>Layer six</i>	<i>slag or stone</i>		20	

2.2. Design of experiments

In order to reduce the size of the training database while keeping the sample representative, we used the HAP programme to generate the result, and we have six layers: Layer one has one material and three thicknesses; layer two, the air space, has one thickness for each type of roof; layer three has four materials with three thicknesses for each type of wall; layer four has one material for each type of wall with three thicknesses; and layers 5 and 6 have one material with one thickness for each type of roof. So the number of models created is $(1 \times 3) \times (1) \times (4 \times 3) \times (1 \times 3) \times (1 \times 1) \times (1 \times 1) = 108$ models for one type of roof, and for three roofs, we collect $3 \times 108 = 324$ models. So that we can choose the effective parameters and the parameters that help us choose the type and thickness of a material in the optimization stage.

3. Artificial Neural Network Model

An artificial neural network (ANN) is a computational model that utilises historical data to facilitate self-learning and forecasts future outcomes related to the engine's performance. The primary advantage of artificial neural networks lies in their ability to effectively model the dynamics of nonlinear systems. Thus, it can be inferred that the tool is highly adaptable and efficient in modelling intricate and non-linear problems (Majid et al., 2021).

Neural networks exhibit a conceptual similarity to the human brain. The neural network is composed of a set of processing units known as neurons, along with either linear or nonlinear activation functions. The neural network architecture typically comprises of three layers, namely the input layer, one or more hidden layers, and the output layer. By means of an iterative computation process known as the training process, Artificial Neural Networks can establish a correlation between the inputs and outputs of a given system (Askar et al., 2022). In the process of training, it is possible to adjust the weights and biases assigned to the inputs in order to optimise the outputs and minimise inaccuracies, thereby achieving the desired objective (Jaber et al., 2019).

3.1. Data preparation

In this work, we used HAP software to create roof models and calculate heat loss for each model. We assumed that the cost of the heat loss added to the volume of each layer is a unit price. The objectives were heat loss, cost, and overall heat transfer coefficient. The input data consisted of 12 parameters: the resistance and the dimension of each layer, with six parameters for each, to generate data sets that are required for the training process of an artificial neural network (ANN). The collected data underwent normalisation to conform to the range of [0.1–0.9], which corresponds to the minimum and maximum values of the data. The process of normalisation is deemed crucial in achieving optimal fitting within a shorter time (Neelamegam and Arasu, 2016).

3.2. Neural network architecture

The roof model performance prediction is conducted by using a neural network model with a two-layer feedforward network (nftool-MATLAB). As shown in Fig. 2 and 3, the network structure includes 12 input layers, a ten-neuron hidden layer with a sigmoid transfer function, and an output layer with a purelin transfer function. The employed inputs to the network were 12: six are the resistance for each layer (R1–R6) and the other six are the thickness dimension for each layer (Th.1–Th.6). While the outputs were the heat loss (Q), the cost of the model (Cost) and overall heat transfer coefficient (U).

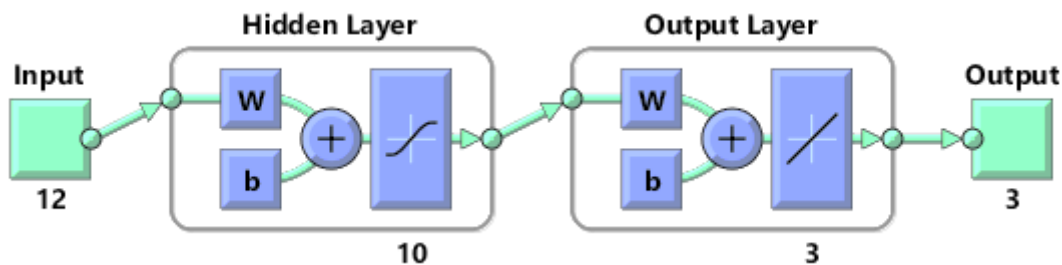


Figure 2. Schematic of the architecture neural network model

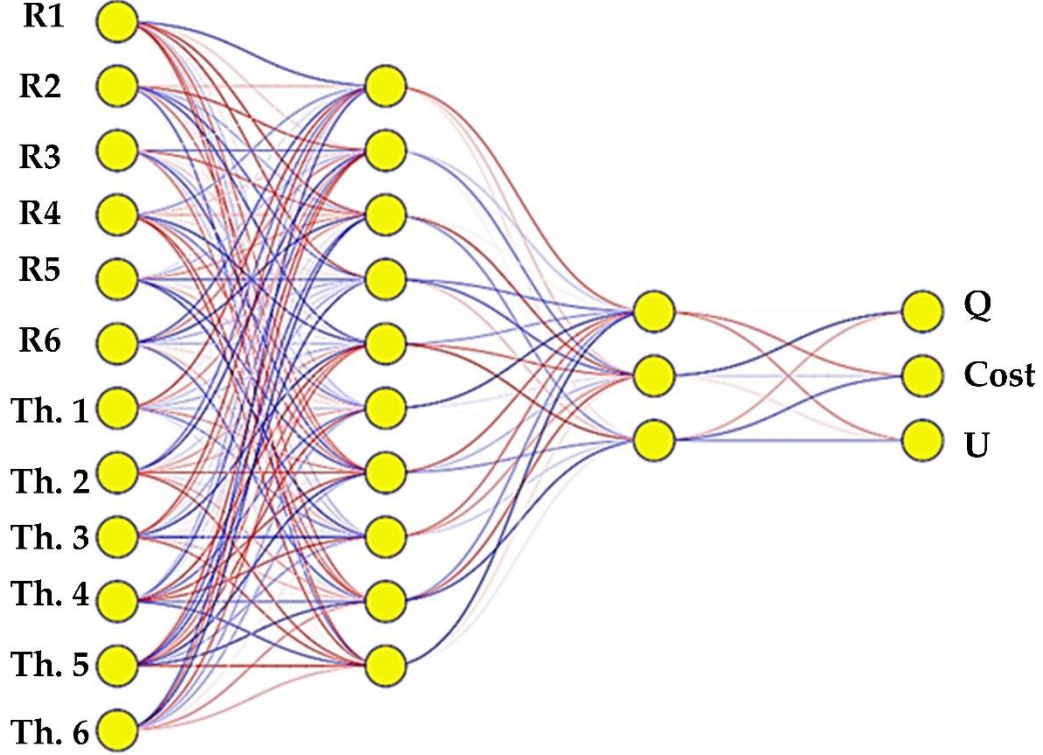


Figure 3. Schematic of the neural network model architecture

3.3. Training

The suggested network is trained using data obtained through experimental computations. The normalised dataset is then randomly split into three parts: the training set (70 percent), the validation set (15 percent), and the testing set (15 percent). Levenberg–Marquardt backpropagation (LM) was employed as a learning method throughout the training phase, and performance was measured using mean squared error (MSE) (Xue et al., 2019). In Eq. 1 a decrease in MSE indicates high predictive performance, similar to the results of the analytical model. A strong correlation was observed when R (Askar et al., 2022) approaches unity in Eq. 2, indicating a strong correlation between the analytical model results and the ANN forecast outputs. The process of training persists through multiple iterations, referred to as epochs, until the intended outcomes are attained. The epoch count denotes the number of times that the network processes all of the training samples. As a result, modifications are implemented to the neuronal weights and biases during the initial phase of every epoch, as indicated by sources (Moradzadeh et al., 2020). The MSE performance of the network throughout training, validation and testing is shown in Fig. 4.

$$MSE = \frac{\sum_{i=1}^n (a_{N,i} - p_{N,i})^2}{n}, \quad (1)$$

$$R^2 = 1 - \frac{\sum_{i=1}^n (a_i - p_i)^2}{\sum_{i=1}^n (p_i)^2}, \tag{2}$$

where a_i is the actual value and p_i is the predicted value.

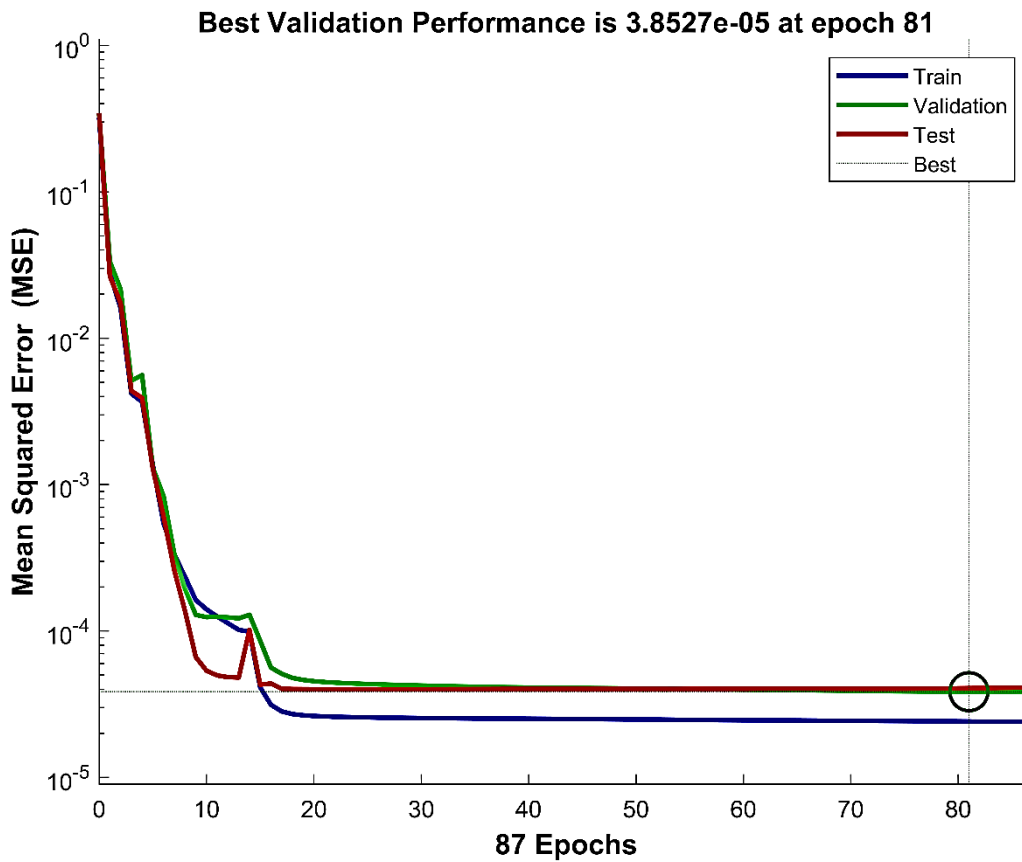


Figure 4. Schematic of the MSE performance of the network with number of iteration

The regression graph (R) shows in Fig. 5 the correlation between the neural network outputs and the system objectives, to indicate that the output variable Y is equal to the target variable T . This means that the regression model is trying to predict the target value as accurately as possible, minimizing the error between Y and T . Ideally, the points should lie close to the diagonal line $Y = T$, indicating a perfect match between the prediction and the target.

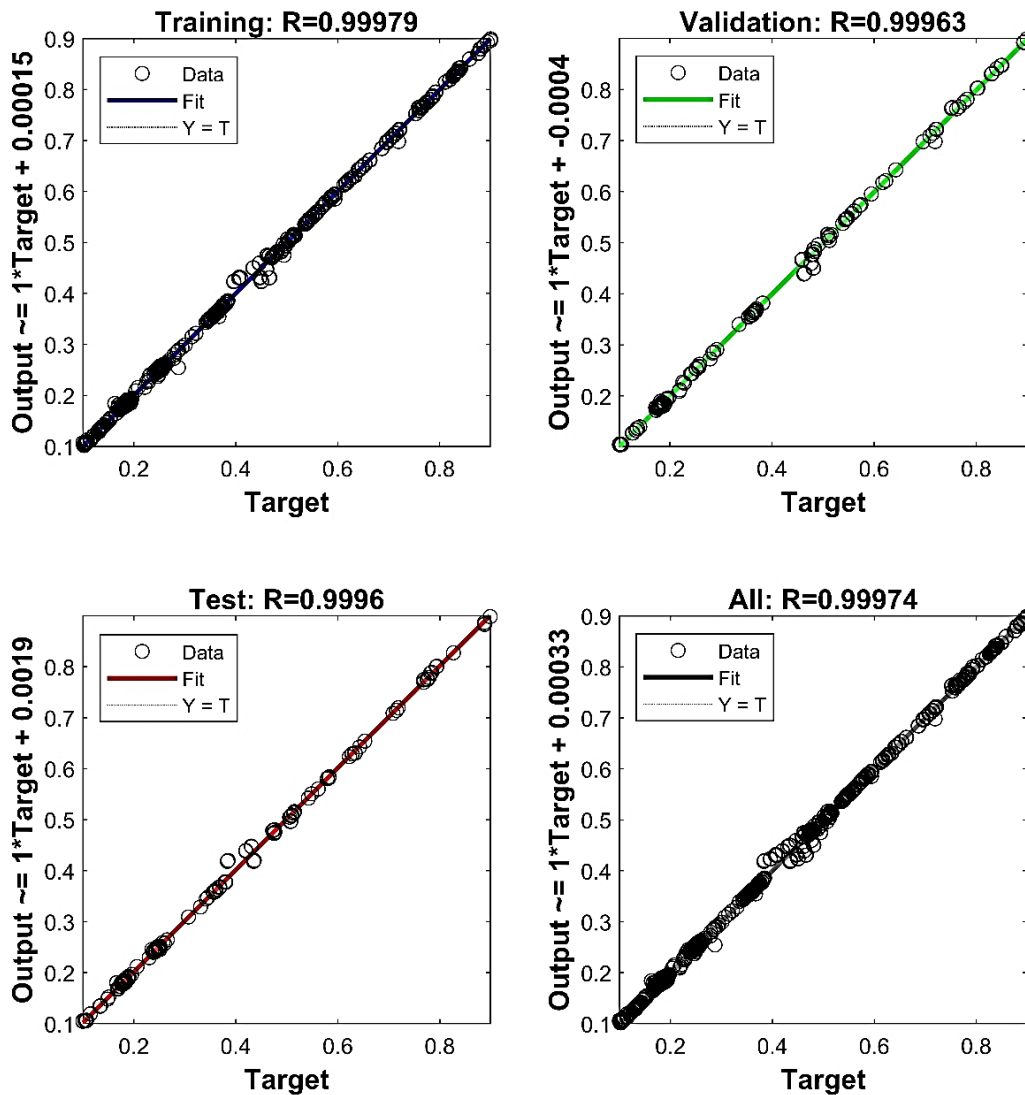


Figure 5. Schematic of the regression graphing (R) for the training, validation, testing and for the all data

3.4. Optimization

The “survival of the fittest” principle in evolutionary biology serves as the inspiration for a multi-objective genetic algorithm, which is a population-based strategy. It uses selection, mutation, and crossover operators, innovative fitness functions, and tactics to enhance feasible solutions (Long et al., 2015). A multi-objective genetic algorithm optimization method is a technique that can find a set of optimal solutions for problems that have more than one objective or criterion. For this research, we want to design a roof that reduces heat loss and costs. We have two conflicting objectives that need to be balanced. A multi-objective genetic algorithm can help to find a set of trade-off solutions that are optimal in some sense.

3.4.1. Multi-objective optimization

Multi-objective optimization (MOO) models capture the multiple, frequently conflicting, and often incommensurable parts of solution evaluation to reveal trade-offs and provide a technological framework for decision-making. MOO frequently has many non-dominated (Pareto optimum) solutions rather than one optimal one due to conflicting goals. We limit heat loss and costs. Roof performance calculations make this MOO model combinatorial and nonlinear. Thus, a multi-objective genetic algorithm (MOGA) defines the front neutral zone. Within MOGA, the ANN analyses heat loss and cost, while the ‘gamultiobj’ function of the Genetic Algorithm (GA) toolbox in MATLAB performs the optimization.

3.4.2. Decision variables

The decision variables reflect the total set of alternative measures that are available for flooring retrofitting (Albedran and Askar, 2021) (e.g. type of material, thickness of the material, etc.). The set of retrofit actions concerns combinations of choices regarding material of layers, Acoustic tile, Ceiling air space, concrete, insulation, felt and membrane, and slag or stone and different thicknesses for each layer. Twelve types of decision variables are defined concerning the alternative choices regarding: six thermal resistance of layers and six thickness of layers.

3.4.3. Objective functions

3.4.3.1. Heat loss

The heat loss of the roofing is directly assessed by HAP. The total heat loss, consists in the sum of energy losses through the layers, and its based on the equation:

$$Q = UA(T_i - T_o), \quad (3)$$

where U is the overall heat transfer coefficient [W/m^2K], A is the area of the roof [m^2], and T_i , T_o are the inside and outside temperature [K].

After training the neural network model, the MOGA uses the ANN model to calculate optimum heat loss.

3.4.3.2. Cost

The overall investment cost for the roof is Cost (X), where X denotes the vector of all decision variables defined, and we can calculate it according to the dimension of the type of roof and the heat loss. It is denoted by a unit price for the unit volume of each layer and heat loss.

3.4.3.3. Optimal

We employed the Genetic Algorithm (GA) after we created the neural network using the data to identify the Pareto set for the Multi-Objective Optimisation (MOO) problem see Fig. 6. The Pareto set comprises a collection of solutions that satisfy the objectives, but further analysis is required to ascertain the most favourable choice (Duan et al., 2014). Therefore, we used the Improved Minimum Distance Selection Method (IMDSM) (Chen et al., 2017) to standardise the Pareto solutions and identify the optimal solution, or the “knee point”, which can be expressed in Eq. 4. Then, we can specify the optimal roof model. The result for the optimal roof model is shown in Table 2.

$$D_{min} = \sqrt{\sum_{\tau=1}^n \left(\frac{f_{c\tau}(x)}{\min(f_{\tau}(x))} - 1 \right)^2} \tag{4}$$

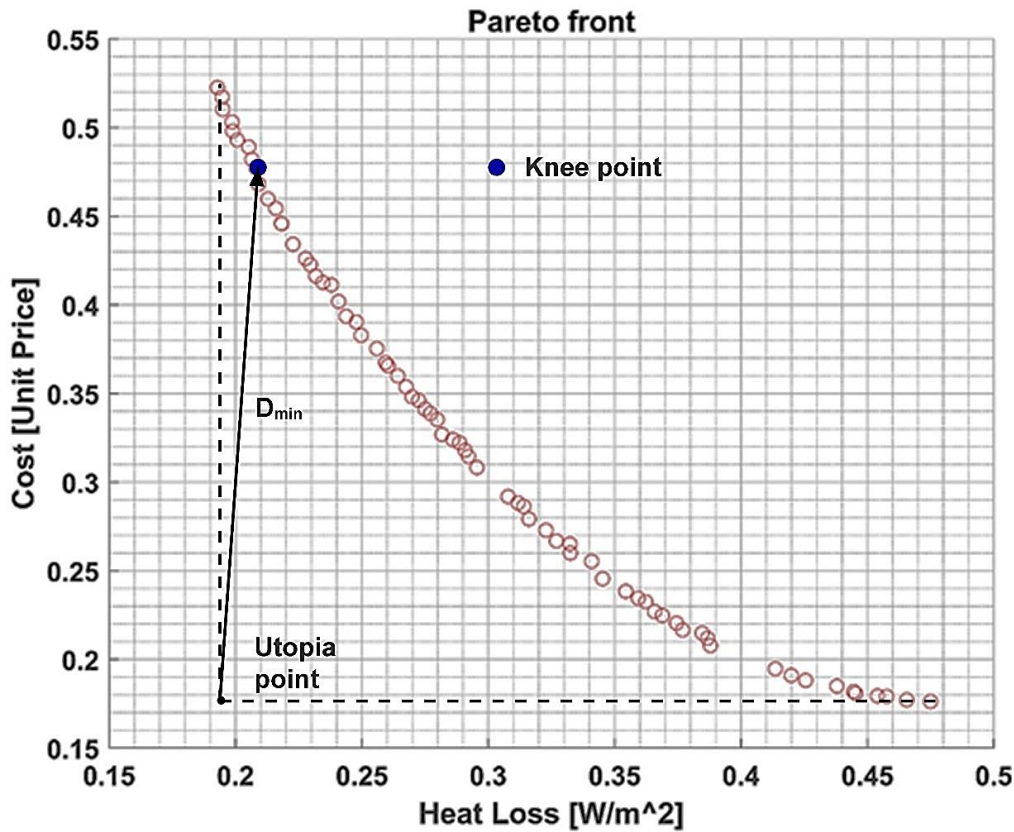


Figure 6. The optimal solutions and knee points of the Pareto optimal front

Table 2. The properties and thickness of the optimal roof layers

	Acoustic tile	Ceiling air space	HW concrete	insulation	felt and membrane	slag or stone
K [W/m K]	0.2877	0.4116	0.2997	0.1017	0.1361	1.3318
P [kg/m ³]	480.6	1.1	977.1	8.0	1121.3	881.0
C_p [J/kg K]	840	1.007	840	840	1670	1670
Thickness [mm]	30	20	150	100	15	15

3.5. Ansys simulation

In this study, we performed the transient thermal analysis in Ansys because it is available and gives us good results for this problem of the optimal roof with convection and radiation heat transfer at the inside comfortable zone and outside environment. We used Ansys Workbench finite element analysis (FEM)

of the heat transfer and temperature distribution in a roof subjected to convection and radiation. The objective is to investigate the heat loss of the optimal roof and compare it with the heat loss of HAP and ANN. We assumed that the problem is transient thermal with constant thermal properties (see table 2). Figure 7 shows the geometry and mesh of the optimal roof model, we take the problem for 1 meter square area: the length and the width are 1 m. The thickness of the layers see table 2. The quadratic mesh element size is 0.03 m, the number of element is 13068 and 75072 nodes.

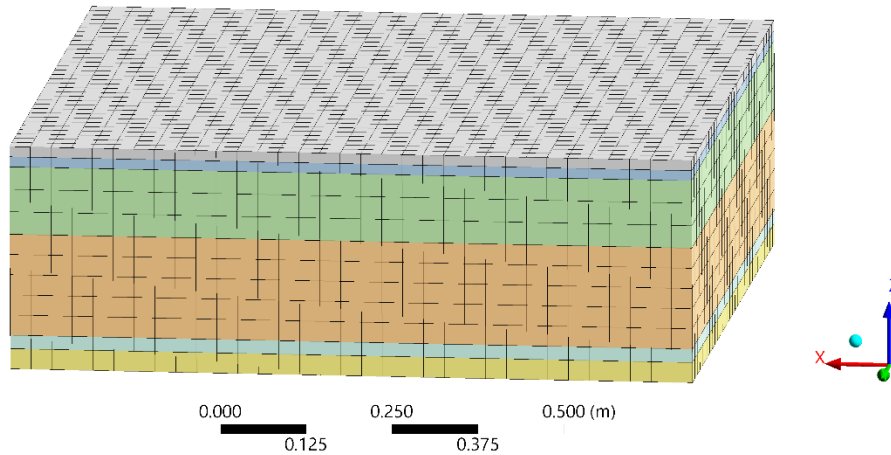


Figure 7. Geometry and mesh of the optimal roof model.

The initial and boundary conditions are shown in Table 3. It is taken from the HAP programme for the weather data of Miskolc city for design day in January. As you can see, the interior condition is a comfortable zone; it is a constant condition, and the exterior condition is changing with time.

Table 3. The initial and boundary conditions for simulation case optimal roof

h_i [W/m ² K]	h_o [W/m ² K]	T_i [K]	T_o [K]	ϵ	$T_{initial}$ [K]
8.289	13–17	295	269–279	0.9	288

To perform the transient thermal analysis, we used Ansys Mechanical APDL solver and set the convergence criterion to 0.0001 °C for the maximum change in nodal temperature per iteration. Then we postprocessed the results with Ansys Workbench.

4. Results and discussion

The results for the data of the roof for HAP and ANN models, as we can see in Fig. 8, illustrate the values of the experimental data heat loss and the trained data per model number obtained through the Levenberg–Marquardt backpropagation. As stated earlier, the main reason for employing training data and test data as well as comparing them is to prove the accuracy and reliability of the analysis conducted in this research and to use this function in the optimization method. It can be shown that the network has a very good match with the system.

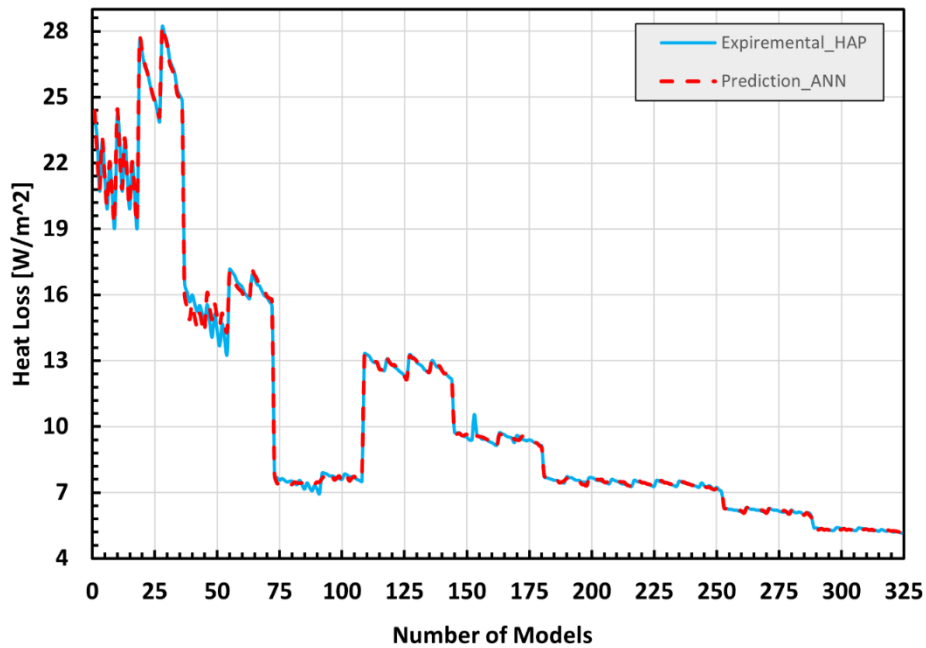


Figure 8. Experimental and prediction heat loss with number of models

Figure 9 shows the temperature distribution along the roof thicknesses when the maximum heat loss occurred. It can be seen that the temperature transferred from the inside to the outside due to heat loss by convection and radiation.

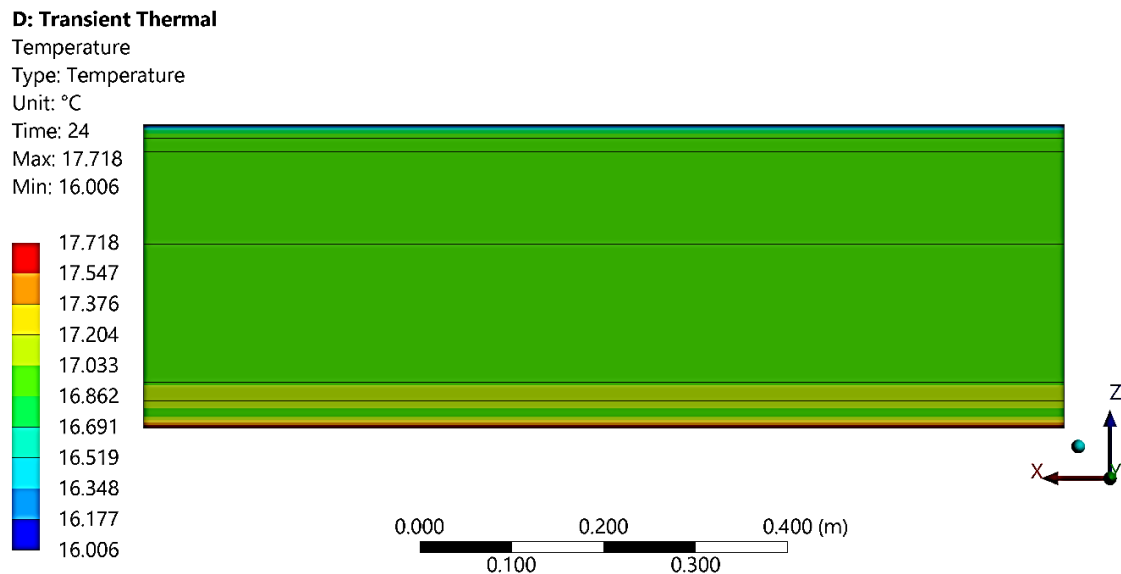


Figure 9. Temperature distribution along the roof thicknesses

Finally we can present Table 4 for the heat loss through the roof to compare between three type of solvers after make optimization, and the difference between the solvers is HAP to ANN and ANSYS, and the difference between the last two solvers is (0.013, -0.01 , and -0.023%), respectively.

Table 4. The heat loss through the roof

	HAP	ANN	ANSYS
Heat loss [W/m ²]	12.28	12.12	12.413

5. Conclusion

This paper presents a study of the heat loss through the roof in winter season at Miskolc, Hungary, for various roof models with the goal of reducing energy consumption, heat loss, and gas emissions in cold regions. We created several models using HAP software and collected the data. We then used the data to train an artificial neural network and applied a multi-objective genetic algorithm to find the optimal model. We also performed a transient thermal analysis using Ansys and compared the results with the optimal model, which were 12.28, 12.12, and 12.413 W/m² for HAP, ANN, and transient thermal analysis by Ansys, respectively. And in our next work, we will study the other type of roof, the inclined roof.

References

- [1] Zingre, K. T., Yang, E., and Pun, M. (2017). Dynamic thermal performance of inclined double-skin roof: Modeling and experimental investigation. *Energy*, 133, pp. 900–912. <https://doi.org/10.1016/j.energy.2017.05.181>
- [2] Al-Sanea, S. A. (2002). Thermal performance of building roof elements. *Building and Environment*, 37(7), pp. 665–675. [https://doi.org/10.1016/S0360-1323\(01\)00077-4](https://doi.org/10.1016/S0360-1323(01)00077-4)
- [3] Höglund, B. I., Mitalas, G. P., Stephenson, D. G. (1967). Surface temperatures and heat fluxes for flat roofs. *Building Science*, 2(1), pp. 29–36. [https://doi.org/10.1016/0007-3628\(67\)90005-9](https://doi.org/10.1016/0007-3628(67)90005-9)
- [4] Imran, H. M., Kala, J., Ng, A. W. M., and Muthukumaran, S. (2018). Effectiveness of green and cool roofs in mitigating urban heat island effects during a heatwave event in the city of Melbourne in southeast Australia. *Journal of Cleaner Production*, 197(1), pp. 393–405. <https://doi.org/10.1016/j.jclepro.2018.06.179>
- [5] Wilkes, K. E., Petrie, T. W., Atchley, J. A., and Childs, P. W. (1997). Roof heating and cooling loads in various climates for the range of solar reflectances and infrared emittances observed for weathered coatings. *Commercial Buildings: Technologies, Design, and Performance Analysis*, June, pp. 361–372.
- [6] Petter, B., Edsjø, S., and Gao, T. (2015). Low-emissivity materials for building applications: A state-of-the-art review and future research perspectives. *Energy Build.*, 96(7491), pp. 329–356. <https://doi.org/10.1016/j.enbuild.2015.03.024>
- [7] Chen, J. and Lu, L. (2021). Comprehensive evaluation of thermal and energy performance of radiative roof cooling in buildings. *J. Build. Eng.*, 33(January), p. 101631. <https://doi.org/10.1016/j.jobe.2020.101631>
- [8] Santamouris, M., Synnefa, A., and Karlessi, T. (2011). Using advanced cool materials in the urban built environment to mitigate heat islands and improve thermal comfort conditions. *Sol. Energy*, 85(12), pp. 3085–3102. <https://doi.org/10.1016/j.solener.2010.12.023>.

- [9] Hong, C. *et al.* (2022). Is the design guidance of color and material for urban buildings a good choice in terms of thermal performance? *Sustain. Cities Soc.*, 83(January), p. 103927. <https://doi.org/10.1016/j.scs.2022.103927>
- [10] Nowak, H. (1991). The longwave radiative heat transfer building envelopes. *Infrared Physics*, 32, pp. 357–363, [https://doi.org/10.1016/0020-0891\(91\)90124-X](https://doi.org/10.1016/0020-0891(91)90124-X).
- [11] Shi, Z. and Zhang, X. (2011). Analyzing the effect of the longwave emissivity and solar reflectance of building envelopes on energy-saving in buildings in various climates. *Sol. Energy*, 85(1), pp. 28–37, <https://doi.org/10.1016/j.solener.2010.11.009>.
- [12] Chantawong, P. (2017). Field-measured performance of lightweight roof chimney integrated with DC fans. *Energy Procedia*, 138, pp. 44–49, <https://doi.org/10.1016/j.egypro.2017.10.044>.
- [13] Carrier company, Hourly Analysis Program, *Building load calculation & energy-modeling software*. Accessed: Jun. 01, 2023. [Online]. Available: <https://www.carrier.com/commercial/en/us/software/hvac-system-design/hourly-analysis-program/>
- [14] Kho, S., Baker, C., and Hoxey, R. (2002). POD / ARMA reconstruction of the surface pressure field around a low rise structure. *Journal of Wind Engineering and Industrial Aerodynamics*, 90(12–15), pp. 1831–1842, [https://doi.org/10.1016/S0167-6105\(02\)00291-X](https://doi.org/10.1016/S0167-6105(02)00291-X).
- [15] Moayed, H., Bui, D. T., Dounis, A., Lyu, Z., and Foong, L. K. (2019). Predicting heating load in energy-efficient buildings through machine learning techniques. *Applied Sciences*, 9(20), p. 4338, <https://doi.org/10.3390/app9204338>.
- [16] Lu, G. Y. and Wong, D. W. (2008). An adaptive inverse-distance weighting spatial interpolation technique. *Computers & Geosciences*, 34(9), pp. 1044–1055. <https://doi.org/10.1016/j.cageo.2007.07.010>
- [17] Jang, J., Baek, J., and Leigh, S.-B. (2019). Prediction of optimum heating timing based on artificial neural network by utilizing BEMS data. *J. Build. Eng.*, 22, pp. 66–74. <https://doi.org/10.1016/j.jobe.2018.11.012>
- [18] Gardner, M. W., and Dorling, S. R. (1998). Artificial neural networks (the multilayer perceptron) – A review of applications in the atmospheric sciences. *Atmospheric Environment*, 32(14–15), pp. 2627–2636, [https://doi.org/10.1016/S1352-2310\(97\)00447-0](https://doi.org/10.1016/S1352-2310(97)00447-0).
- [19] Pandey, S., Hindoliya, D. A., and Mod, R. (2012). Artificial neural networks for predicting indoor temperature using roof passive cooling techniques in buildings in different climatic conditions. *Appl. Soft Comput. J.*, 12(3), pp. 1214–1226. ISBN9827242962. <https://doi.org/10.1016/j.asoc.2011.10.011>
- [20] Tausendschön, J. and Radl, S. (2021). Deep neural network-based heat radiation modelling between particles and between walls and particles. *International Journal of Heat and Mass Transfer*, 177, p. 121557, <https://doi.org/10.1016/j.ijheatmasstransfer.2021.121557>.
- [21] Gao, M. (2022). An artificial neural network-based approach to optimizing energy efficiency in residential buildings in hot summer and cold winter regions. *Computational Intelligence and Neuroscience*, 2022, p. 2611695, <https://doi.org/10.1155/2022/2611695>.
- [22] Askar, A. H., Albedran, H., Kovács, E., and Jármai, K. (2021). A new method to predict temperature distribution on a tube at constant heat flux. *Multidiszcip. Tudományok*, 11(5), pp. 363–372, <https://doi.org/10.35925/j.multi.2021.5.40>.
- [23] Majid, I. L., Saleh, A. A. M., and Jaber, A. A.: *Prediction of refrigeration system performance using artificial neural networks*. ICYRIME 2021, International Conference of Yearly Reports on Informatics Mathematics and Engineering, online, vol. 3118, pp. 90–98.

- [24] Askar, A. H., Kovács, E., and Bolló, B. (2022). ANN modeling for thermal load estimation in a cabin vehicle. *Vehicle and Automotive Engineering 4: Select Proceedings of the 4th VAE2022, Miskolc, Hungary*, Springer, pp. 357–373, https://doi.org/10.1007/978-3-031-15211-5_31.
- [25] Jaber, A. A., Saleh, A. A. M., and Ali, H. F. M. (2019). Prediction of hourly cooling energy consumption of educational buildings using artificial neural network. *International Journal on Advanced Science, Engineering and Information Technology*, 9(1), pp. 159–166. <https://doi.org/10.18517/ijaseit.9.1.7351>
- [26] Neelamegam, P. and Arasu, V. (2016). Prediction of solar radiation for solar systems by using ANN models with different back propagation algorithms. 14, pp. 206–214. <https://doi.org/10.1016/j.jart.2016.05.001>
- [27] Xue, G., Pan, Y., Lin, T., Song, J., Qi, C. and Wang, Z. (2019). District heating load prediction algorithm based on feature fusion LSTM model. *Energies*, 12(11), p. 2122. <https://doi.org/10.3390/en12112122>
- [28] Moradzadeh, A., Mansour-Saatloo, A., Mohammadi-Ivatloo, B., and Anvari-Moghaddam, A. (2020). Performance evaluation of two machine learning techniques in heating and cooling loads forecasting of residential buildings. *Applied Sciences*, 10(11), p. 3829. <https://doi.org/10.3390/app10113829>
- [29] Long, Q., Wu, C., Wang, X., Jiang, L., and Li, J. (2015). A multiobjective genetic algorithm based on a discrete selection procedure. *Mathematical Problems in Engineering*, 2015, p. 349781, <https://doi.org/10.1155/2015/349781>.
- [30] Albedran, H. and Askar, A. H. (2021). Interpolated spline method for a thermal distribution of a pipe with a turbulent heat flow. *Multidiszciplináris Tudományok*, 11(5), pp. 353–362. <https://doi.org/10.35925/j.multi.2021.5.39>
- [31] Duan, S., Tao, Y., Han, X., Yang, X., Hou, S., and Hu, Z. (2014). Investigation on structure optimization of crashworthiness of fiber reinforced polymers materials. *Compos. Part B*, 60, pp. 471–478, <https://doi.org/10.1016/j.compositesb.2013.12.062>.
- [32] Chen, Y., Liu, G., Zhang, Z., and Hou, S. (2017). Integrated design technique for materials and structures of vehicle body under crash safety considerations. *Structural and Multidisciplinary Optimization*, 56, pp. 455–472, <https://doi.org/10.1007/s00158-017-1674-8>.